Structural Effects in High-Temperature Electrooptic Chromophores

S. Yamada,[‡] R. F. Shi,*[,†] Y. M. Cai,[†] O. Zamani-Khamiri,[†] A. Panackal,[†] and A. F. Garito[†]

Department of Physics and Astronomy and Department of Materials Science and Engineering University of Pennsylvania Philadelphia, Pennsylvania 19104

Received May 29, 1996
Revised Manuscript Received August 7, 1996

Organic and polymeric systems have been the subject of intense research in recent years due to their potential applications in optoelectronic devices.[1−4] Until recently, materials developments have mainly centered on poly(methyl methacrylate) (PMMA) based polymer matrixes and on substituted stilbenes as the nonlinear optical chromophores. The low glass transition temperature (T_g) of PMMA and the low decomposition temperature of the chromophores have, however, severely limited their usefulness in device applications. Attention has now turned to the use of polyimides, a class of high-T_g polymers well-known in microelectronic industry, as the polymer matrix in optoelectronic devices.[5−7] Earlier, we had reported the design and synthesis of a new class of high-temperature electrooptic (EO) chromophores that may be suitable for use in polyimide-based optical device technology.[8,9] These new chromophores possess relatively large second-order optical coefficients as well as high thermal, chemical, and photo stabilities. In the process of optimizing these structures, we found that isomers which have very similar molecular structures exhibit marked differences in both their linear and nonlinear optical properties. We report here theoretical and experimental results of structural isomer effects on second-order optical susceptibilities,[10] as evidenced in the case of our high-temperature EO chromophores.

The structures of our model systems, 1,8-naphthoylene-(3′-amino) benzimidazole-4,5-dicarbox-*N*-(2,5-di-*tert*-butyl)phenylimide (SY177) and its isomer 1,8-naphthoylene-(4′-amino)benzimidazole-4,5-dicarbox-*N*-(2,5-di-*tert*-butyl)phenylimide (SY177P) are shown in Figure 1 (inset). They differ only in the position of the substitution site of the amine (NH_2) electron donor group. Despite their strong structural similarity, their optical spectra are very different as shown in Figure 1. As described below, the origin of the difference resides in the finding that the first excited state (S_1) of SY177, which is 2.21 eV (562 nm) above the ground state (S_0), is strongly coupled to S_0. In contrast, for SY177P, the coupling between S_1 and S_0 states is very weak. It is the second excited state S_2 in SY177P, 2.91 eV (427 nm) above the ground state S_0, on the other hand, that is found to be strongly coupled to the S_0 state. This finding further suggests that the two isomers should have very different second-order optical properties.

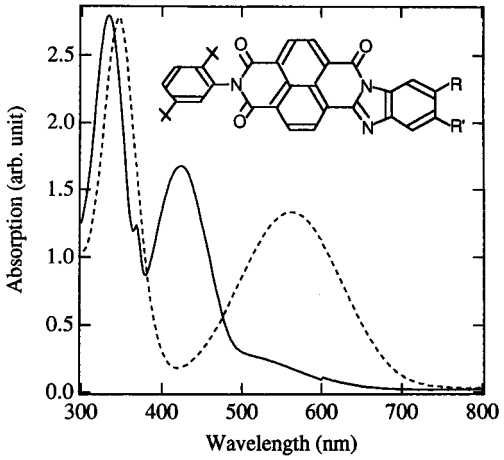

Figure 1. Linear absorption spectra for SY177 (dashed curve) and SY177P (solid curve) in solution with 1,4-dioxane. Inset: schematic molecular structure diagram of SY177 (R = NH_2, R′ = H) and SY177P (R = H, R′ = NH_2).

Table 1. Calculated Transition Moments, Dipole Moments Difference, and Transition Energies in the Gas Phase between Key States for SY177 and SY177P

structure	$\mu^x_{S_1S_0}$ (D)	$\Delta\mu^x_{S_2S_0}$ (D)	$\mu^x_{S_2S_0}$ (D)	$\Delta\mu^x_{S_2S_0}$ (D)	$E_{S_1S_0}$ (eV)	$E_{S_2S_0}$ (eV)
SY177	7.15	12.38	1.33	5.65	2.44	3.32
SY177P	0.50	16.03	6.63	5.08	2.45	2.94

Earlier, we reported that quantum many-electron calculations provide a highly accurate description of the optical and nonlinear optical properties of these high-temperature chromophores such as SY177.[8] In this study, the calculations were extended to SY177P. The twisted phenyl ring in the actual structures, which contributes little to the overall nonlinear optical processes, is replaced by a hydrogen atom to keep the study focused on the important features and to simplify the calculations. The *x* axis is the long molecular axis. It is found that for both SY177 and SY177P, the ground state S_0 is dominantly composed of the ground configuration χ_0, in which all molecular orbitals below the Fermi level are occupied, whereas for the first excited state S_1, a single configuration, in which one electron from the highest occupied molecular orbital (π_0, HOMO) is excited to the lowest unoccupied molecular orbital (π^*_0, LUMO), contributes overwhelmingly. However, as shown in Table 1, while the coupling between S_1 and S_0 states in SY177 is strong, with an *x* component of the transi-

[†] Department of Physics and Astronomy.
[‡] Department of Materials Science and Engineering.

(1) Franke, H. In *Polymers for Lightwave and Integrated Optics: Technology and Applications*; Hornak, L. A., Ed.; Marcel Dekker: New York, 1992; pp 207−230.
(2) Garito, A. F.; Shi, R. F.; Wu, M. H. *Phys. Today* **1994**, *47* (5), 51.
(3) Binkley, E. S.; Nara, S. In *Organic Thin Films for Photonic Applications Technical Digest*; Optical Society of America: Washington, DC, 1993; Vol. 17, pp 266−269.
(4) Matsuura, T.; Ando, S.; Sasaki, S.; Yamamoto, F. *Macromolecules* **1994**, *27*, 6665.
(5) Wu, J. W.; Binkley, E. S.; Kenney, J. T.; Lytel, R.; Garito, A. F. *J. Appl. Phys.* **1991**, *69*, 7366.
(6) Kowalczyk, T. C.; Kosc, T. Z.; Singer, K. D.; Cahill, P. A.; Seager, C. H.; Meinhardt, M. B.; Beuhler, A.; Wargowski, D. A. *J. Appl. Phys.* **1994**, *76*, 1111.
(7) Verbiest, T.; Burland, D. M.; Jurich, M. C.; Lee, V. Y.; Miller, R. D.; Volksen, W. *Science* **1995**, *268*, 1604.
(8) Shi, R. F.; Wu, M. H.; Yamada, S.; Cai, Y. M.; Garito, A. F. *App. Phys. Lett.* **1993**, *63*, 1173.
(9) Yamada, S.; Cai, Y. M.; Shi, R. F.; Wu, M. H.; Garito, A. F. *Mater. Res. Soc. Proc.* **1994**, *328*, 523.
(10) Shi, R. F.; Yamada, S.; Cai, Y. M.; Zamani-Khamiri, O.; Panackal, A.; Garito, A. F. In *Quantum Electronics Conference*; Optical Society of America: Washington, DC, 1995; Vol. 16, 1995 OSA Technical Digest Series, pp 137.
(11) Heflin, J. R.; Wong, K. Y.; Zamani-Khamiri, O.; Garito, A. F. *Phys. Rev.* **1988**, *B38*, 1573.

S0897-4756(96)00303-1 CCC: $12.00

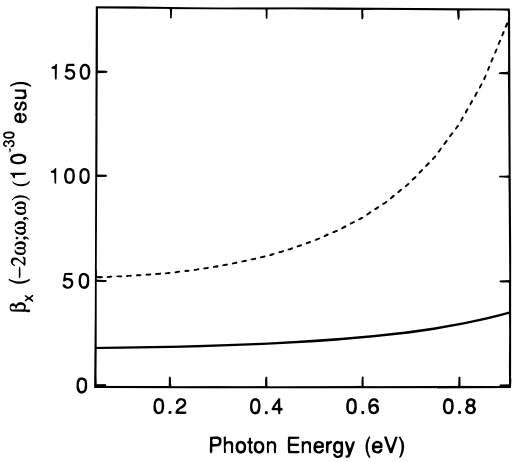

Figure 2. Calculated dispersion curves of $\beta_x(-2\omega;\omega,\omega)$ for SY177 (dashed curve) and SY177P (solid curve).

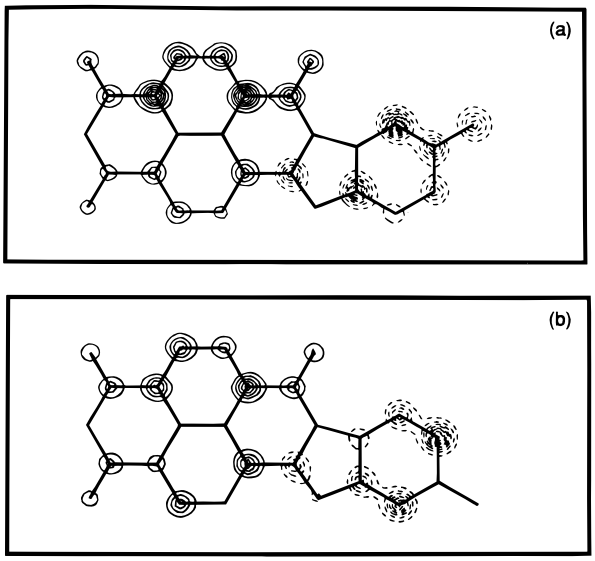

Figure 3. Contour diagrams of the electron charge density distribution difference between (a) the S_0 and S_1 electronic states for SY177 and (b) the S_0 and S_2 electronic states for SY177P. Solid lines and dashed lines correspond to increased and decreased charge density, respectively, and the contour cut is taken at 0.4 Å above the molecular plane. The dipole moment differences are 12.38 D for SY177 and 5.08 D for SY177P.

tion dipole moment $\mu^x_{S_1S_0} = 7.15$ D, the coupling between S_1 and S_0 states in SY177P is much weaker, with $\mu^x_{S_1S_0} = 0.50$ D. The second excited state S_2 in SY177P, which was found to mainly consist of excitations from the second highest occupied orbital π_{-1} to LUMO π^*, is by contrast strongly coupled to the ground state S_0. These results agree well with the measured optical absorption spectra shown in Figure 1 in both the transition energies and overall features.

Figure 2 shows the calculated dispersion results of $\beta_x(-2\omega;\omega,\omega)$, the dominant vector part of β_{ijk}, for SY177 and SY177P as a function of input photon energy. All the transition energies for both systems were properly displaced[8] to account for solute−solvent interactions. We note that over the entire nonresonant region, the value of $\beta_x(-2\omega;\omega,\omega)$ for SY177P is much smaller than that for SY177. The reason is that in SY177, the largest contribution to $\beta_x(-2\omega;\omega,\omega)$ is a virtual transition sequence involving only two states S_0 and S_1, in the form of $S_0 \rightarrow S_1 \rightarrow S_1 \rightarrow S_0$. While in SY177P, the corresponding sequence is in the form of $S_0 \rightarrow S_2 \rightarrow S_2 \rightarrow S_0$. The smaller dipole moment difference (5.08 D) and the higher transition transition energy (2.94 eV) between the key states (S_0 and S_2) in SY177P combine to result in a smaller second-order optical response. At $\lambda = 1907$ nm (0.65 eV), it was calculated that $\beta_x(-2\omega;\omega,\omega) = 93 \times 10^{-30}$ esu for SY177, which is compared to $\beta_x(-2\omega;\omega,\omega) = 25 \times 10^{-30}$ esu for SY177P.

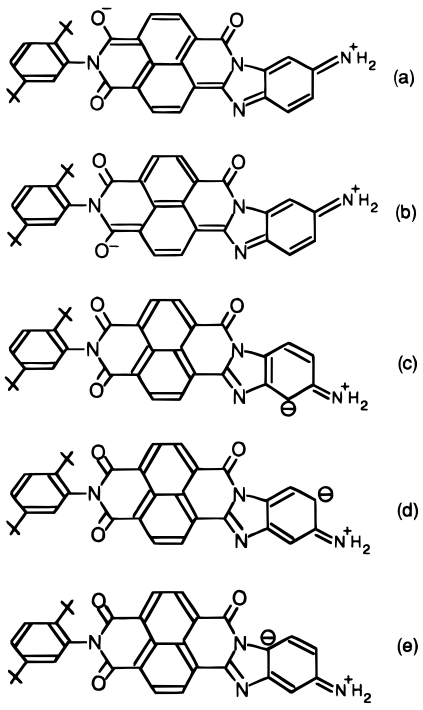

Figure 4. Possible resonance structures for SY177 (a) and (b) and SY177P (c), (d), and (e).

Table 2. Experimental Dipole Moments, Experimental Values of $\mu\beta_x(-2\omega;\omega,\omega) + \langle\gamma(-2\omega;\omega,\omega,0)\rangle 5kT$, and Experimental and Calculated Values of $\beta_x(-2\omega;\omega,\omega)$ at λ = 1907 nm ($\hbar\omega$ = 0.65 eV) for SY177 and SY177P

structure	SY177	SY177P
μ (D)	3.6	3.6
$(\mu\beta + \langle\gamma\rangle 5kT)^{exp}$ (10^{-48} esu)	413	85
β_x^{exp} (10^{-30} esu)	93	21
β_x^{calc} (10^{-30} esu)	93	25

These marked differences can be directly understood by comparing the contour diagrams of the electron density distribution difference between the ground state and key excited state for each model structure. As shown in Figure 3a, for SY177, upon virtual excitation, charge is clearly separated from the NH_2 donor group across the length of the chromophore to the imide acceptor region leading to a large dipole moment difference of 12.38 D. In contrast, as shown in Figure 3b for SY177P, the NH_2 region is not even involved and the charge separation occurs over a shorter length and to a lesser degree. The key transition moments for SY177 are also found to be larger than those for SY177P. These results further demonstrate that computer-aided designs and simulations are able to provide us with microscopic design rules for the EO chromophores prior to the actual material synthesis.

Dc-induced second harmonic generation (DCSHG) measurements using 1,4-dioxane as the solvent were performed to determine the microscopic second-order $\beta_x(-2\omega;\omega,\omega)$ of the two isomers at $\lambda = 1907$ nm (0.65 eV).

The results are summarized in Table 2. The value obtained for $\mu\beta_x(-2\omega;\omega,\omega) + 5\langle\gamma(-2\omega;\omega,\omega,0)\rangle kT$, is 413 $\times 10^{-48}$ esu for SY177 compared to 85 $\times 10^{-48}$ esu for SY177P, both at $\lambda = 1907$ nm. The experimental microscopic $\beta_x(-2\omega;\omega,\omega)$ values are obtained from the $\mu\beta_x(-2\omega;\omega,\omega) + 5\langle\gamma(-2\omega;\omega,\omega,0)\rangle kT$ values using the experimental dipole moments, measured to be 3.6 $\pm$ 0.3 D in both cases and the calculated isotropically averaged third-order susceptibility $\langle\gamma(-2\omega;\omega,\omega,0)\rangle$ for each. The experimental β_x values obtained in this manner are 93 $\times 10^{-30}$ esu and 21 $\times 10^{-30}$ esu for SY177 and SY177P, respectively. The agreement between the experimental and calculated values (Table 2) is quite satisfactory, demonstrating the effectiveness and high reliability of the computer-aided design methods.

As expected, there is a direct correlation between the electron charge densities depicted, for example, in contour diagrams and traditional resonance structures such as those drawn in Figure 4. The resonance representation for SY177 emphasizes the charge separation that spans across the entire molecular structure from the donor NH_2 group to the imide acceptor group. In comparison, in the resonance forms for SY177P, the charge can distribute over only a small section of the molecular structure, reducing the effect of the naphthoylene group that serves as both an electron acceptor and a π-bridge necessary for π-electron delocalization.

In summary, we have carried out a theoretical and experimental study of isomeric structural effects on second-order optical properties for two high-temperature structural isomers, SY177 and SY177P. The results showed that although these isomers are very similar in molecular structure, they differ markedly in second-order nonlinear optical properties. Upon virtual excitation, the electron-donating amine group in SY177 was found to be an active site in the important charge-separation process, while in sharp contrast, the same group in SY177P, positioned differently on an adjacent carbon site, was found to be relatively uninvolved. Dc-induced second harmonic generation measurements confirmed the theoretical predictions, with more than a factor of 4 difference found in the second-order optical responses between these two isomers. The microscopic second-order $\beta_x(-2\omega;\omega,\omega)$ at $\lambda = 1907$ nm (0.65 eV) was measured to be 93 $\times 10^{-30}$ esu for SY177 and 21 $\times 10^{-30}$ esu for SY177P in dioxane solution.

Acknowledgment. This research was generously supported by AFOSR and ARPA (Grant F49620-85-C-0105). The calculations were performed on the CRAY YMP C-90 of the Pittsburgh Supercomputing Center. We are grateful for stimulating discussions with W. D. Chen and M. H. Wu.

CM960303L